Relationship between phosphatidylinositol 4-phosphate synthesis, membrane organization, and lateral diffusion of PI4KIIα at the *trans*-Golgi network

Shane Minogue,* K. M. Emily Chu,* Emily J. Westover,† Douglas F. Covey,† J. Justin Hsuan,* and Mark G. Waugh[1],*

Centre for Molecular Cell Biology,* Department of Inflammation, Division of Medicine, University College London, London, United Kingdom; and Department of Developmental Biology,† Washington University School of Medicine, St. Louis, MO

Abstract **Type II phosphatidylinositol 4-kinase IIα (PI4KIIα) is the dominant phosphatidylinositol kinase activity measured in mammalian cells and has important functions in intracellular vesicular trafficking. Recently PI4KIIα has been shown to have important roles in neuronal survival and tumorigenesis. This study focuses on the relationship between membrane cholesterol levels, phosphatidylinositol 4-phosphate (PI4P) synthesis, and PI4KIIα mobility. Enzyme kinetic measurements, sterol substitution studies, and membrane fragmentation analyses all revealed that cholesterol regulates PI4KIIα activity indirectly through effects on membrane structure. In particular, we found that cholesterol levels determined the distribution of PI4KIIα to biophysically distinct membrane domains. Imaging studies on cells expressing enhanced green fluorescent protein (eGFP)-tagged PI4KIIα demonstrated that cholesterol depletion resulted in morphological changes to the juxtanuclear membrane pool of the enzyme. Lateral membrane diffusion of eGFP-PI4KIIα was assessed by fluorescence recovery after photobleaching (FRAP) experiments, which revealed the existence of both mobile and immobile pools of the enzyme. Sterol depletion decreased the size of the mobile pool of PI4KIIα. Further measurements revealed that the reduction in the mobile fraction of PI4KIIα correlated with a loss of *trans*-Golgi network (TGN) membrane connectivity. We conclude that cholesterol modulates PI4P synthesis through effects on membrane organization and enzyme diffusion.**—Minogue, S., K. M. E. Chu, E. J. Westover, D. F. Covey, J. J. Hsuan, and M. G. Waugh. **Relationship among phosphatidylinositol 4-phosphate synthesis, membrane organization, and lateral diffusion of PI4KIIα at the *trans*-Golgi network. *J. Lipid Res.* 2010.** 51: **2314–2324.**

Supplementary key words PI4P • cholesterol • PI 4-kinase

Phosphatidylinositol 4-phosphate (PI4P) is generated by phosphorylation of phosphatidylinositol (PI) on the 4-position by phosphatidylinositol 4-kinases (1). In mammalian cells (2, 3), PI4P synthesis is predominately accounted for by the type II phosphatidylinositol 4-kinase IIα isoform (PI4KIIα). Our most recent work has shown that loss of PI4KIIα activity in mice leads to late-onset neurodegeneration (2). In addition, Li et al. (4) have demonstrated that PI4KIIα is overexpressed in a wide range of common cancers where it has a key role in promoting angiogenesis. However, despite its emerging importance in disease, little is known about endogenous factors that regulate PI4KIIα, and there are currently no pharmacological reagents available to modulate its activity in cells. We previously demonstrated that PI4KIIα activity is sensitive to membrane cholesterol levels (5). Given the significant role of the enzyme in major pathologies, we sought to investigate the biochemical and biophysical mechanisms that underlie sterol-sensitive PI4P synthesis.

One possible mechanism through which cholesterol could affect PI4KIIα is by modulating its membrane mobility (6–10). Lateral diffusion of a membrane-associated protein determines its interaction dynamics with other membrane components (reviewed in Ref. 6), and in the case of an enzyme such as PI4KIIα, this is likely to be important for the kinetics of product formation. However, it is important to point out that nothing is known

This study was supported by Cancer Research UK Grants C25540/A8562 (M.G.W. and J.J.H.); the Biotechnology and Biological Sciences Research Council Grant BB/G021163/1 (S.M. and M.G.W.); and the National Institutes of Health Grant GM-47969 (D.F.C.). Its contents are solely the responsibility of the authors and do not necessarily represent the official views of the National Institutes of Health or other granting agencies.

Manuscript received 26 January, 2010 and in revised form 13 April 2010.

Published, JLR Papers in Press, April 13, 2010
DOI 10.1194/jlr.M005751

Abbreviations: EGF, epidermal growth factor; eGFP, enhanced green fluorescent protein; FRAP, fluorescence recovery after photobleaching; MβCD, methyl-β-cyclodextrin; PI, phosphatidylinositol; PI4KII, type II phosphatidylinositol 4-kinase; PI4P, phosphatidylinositol 4-phosphate; SUV, small unilamellar vesicle; TGN, *trans*-Golgi network.

[1]To whom correspondence should be addressed.
e-mail: m.waugh@medsch.ucl.ac.uk

about the membrane dynamics of PI4KIIα. Membrane lipid composition and, in particular, membrane cholesterol concentration underlie biophysical parameters such as membrane fluidity, viscosity, and geometry, all of which are known to modulate membrane protein mobility (6). Cholesterol also has a role in the formation and organization of cholesterol-rich microdomains, often referred to as lipid rafts (11, 12), which are proposed to organize membrane signaling events through transient and localized confinement of the relevant signaling molecules (13). The *trans*-Golgi network (TGN) is particularly enriched in cholesterol (14–16) and also contains high levels of PI4P (17–20). These observations have led some authors to suggest that PI4P synthesis is a determinant of TGN organelle identity (21, 22). At the TGN, PI4KIIα activity is required for clathrin-dependent vesicle formation (3, 23). Our main interest is in investigating the relationship between cholesterol and PI4P formation, particularly as the levels of both lipids are important for the formation of trafficking vesicles at the TGN (3, 24–26) and our previous work demonstrated that PI4KIIα activity on intracellular membranes is dependent on membrane sterol levels (5).

The work presented here concerns TGN-associated PI4KIIα as opposed to the endosomal pool of the enzyme (27–31), which has been implicated in AP-3 adaptor recruitment (28, 30, 32). The TGN pool of PI4KIIα corresponds to the juxtanuclear and vesicular PI4KIIα pool that colocalizes with the TGN proteins syntaxin-6 (33) and TGN46 (34) both by microscopy (20, 31, 35) and by subcellular fractionation (36). PI4KIIα is unique among all the PI kinases in that it is constitutively associated with TGN membrane domains (20, 35–37) via post-translational palmitoylation of a central CCPCC motif (35, 38, 39). PI4KIIα palmitoylation is essential for both kinase activity and for localization to the TGN, but this modification is not absolutely required for membrane association of the enzyme (35, 38, 39). Here we focus on regulation of PI4KIIα at the TGN, with particular emphasis on the relationship between membrane organization and lipid composition in regulating PI4KIIα dynamics and activity.

Previously, we established that PI4KIIα and its phospholipid PI substrate associate with buoyant, TGN membrane domains (36) and that all the PI 4-kinase activity associated with these membranes was accounted for by the PI4KIIα isoform (5, 31, 36). Furthermore, we found that PI4P synthesis in these membrane preparations was sensitive to the manipulation of membrane sterol levels by methyl-β-cyclodextrin (MβCD) (5). Cholesterol sequestration by MβCD is often exploited experimentally to disrupt lipid rafts (reviewed in Ref. 40). Using this approach, other groups have shown that agonist-sensitive PI4P pools are MβCD-sensitive (41) and that MβCD delocalizes raft-associated PI4P (42). In addition to lipid raft disruption, cholesterol removal with MβCD is known to induce a more condensed Golgi morphology (43), partial vesicularisation of TGN membranes (24, 44), and changes in the lateral mobility of some TGN-associated proteins (45). However, it is not known how factors, such as membrane domain heterogeneity, TGN membrane continuity, or possible changes to PI4KIIα lateral diffusion, might contribute to the cholesterol-sensitivity of the enzyme. Therefore, in this study we utilize a range of biochemical approaches together with spot photobleaching of enhanced green fluorescent protein (eGFP)-tagged PI4KIIα to elucidate the mechanism underlying cholesterol-dependent PI4P synthesis.

MATERIALS AND METHODS

Materials

Protease inhibitor cocktail tablets (Complete™, without EDTA) were from Roche Diagnostics. Mastoparan was purchased from Calbiochem (Nottingham, UK). MβCD, PI purified from bovine liver, and all the sterols used were bought from Sigma-Aldrich (Poole, Dorset, UK). DMEM, fetal bovine serum, and penicillin/streptomycin were purchased from Invitrogen (Paisley, UK). [γ-^{32}P]ATP (4500–6000 Ci/mmol) was purchased from GE Healthcare. Anti-syntaxin-6 was purchased from BD Pharmingen. Anti-TGN46 was bought from Novus Biologicals. Enantiomeric cholesterol was prepared by catalytic hydrogenation of an enantiomeric desmosterol precursor as described previously (46).

Cell culture

Cells were maintained at 37°C in a humidified incubator at 10% CO_2. Cells were cultured in DMEM supplemented with Glutamax, 10% fetal calf serum, 50 i.u./ml penicillin and 50 μg/ml streptomycin. For fluorescence recovery after photobleaching (FRAP) measurements, cells were transfected 24 h prior to the experiments with eGFP-PI4KIIα.

Subcellular fractionation by sucrose density gradient centrifugation

Post-nuclear supernatants prepared from confluent cell monolayers were fractionated on a 10–40% w/v sucrose density gradient as previously described (5, 31, 36). Buoyant and TGN-enriched membrane fractions 9-10 containing high activity PI4KIIα were harvested as before (5, 31).

Sonication-based assay to fragment PI4KIIα−containing membranes

MβCD (20 mM) was added to an equal volume of TGN membranes (usually 1 ml) on ice for 20 min to give a final MβCD concentration of 10 mM. Then 200 μl of sodium carbonate 1M (pH 11.0) was added. The carbonate-treated membranes were probe sonicated followed by adjustment to 40% sucrose w/v in Tris-HCl 10 mM, EDTA 1 mM, and EGTA 1 mM (pH 7.4) to a final volume of 4 ml. A discontinuous sucrose gradient was formed by overlaying the 40% sucrose layer with 4 ml of sucrose 30% w/v and 4 ml sucrose 5% w/v in Tris-HCl 10 mM, EDTA 1 mM, and EGTA 1 mM (pH 7.4). The gradient was centrifuged overnight at 185,000 *g* at 4°C and 1 ml fractions were harvested beginning at the top of the tube.

Immunoblotting of sucrose density gradient fractions

Equal volume aliquots of density gradient fractions were separated by SDS-PAGE, transferred to PVDF, and probed with anti-PI4KIIα or anti-syntaxin-6 antibodies. Western blots were quantified using image analysis software in Adobe Photoshop CS4.

Determination of cholesterol levels

The cholesterol content of equal volume membrane fractions was assayed using the Amplex red cholesterol assay kit (Molecular Probes).

PI 4-kinase assays

PI 4-kinase assays using either endogenous membrane-associated PI or exogenous PI, and add-back of MβCD complexed sterols were performed as previously described (5, 31, 36). Reaction products were separated by thin layer chromatography and visualized on a Typhoon 9400 phosphorimager (Amersham Biosciences). Quantitative data were obtained within the linear range of the instrument using ImageQuant Software (Amersham Biosciences). Specific PI4KIIα activity associated with each fraction was calculated by dividing the rate of PI4P generation (phosphorimager units/min) by the amount of PI4KIIα protein present in each fraction (arbitrary units) as determined by quantitation of anti-PI4KIIα Western blots. Data analysis and nonlinear regression curve fitting were performed using Prism 5 software (GraphPad, San Diego, CA, USA) and compared using the Student *t*-test where significance was set at $P < 0.05$.

Fluorescence microscopy

Cells were grown on poly(L)lysine-coated glass coverslips for 24 h and then fixed in 4% formaldehyde for 10 min on ice. Cells were permeabilized in 0.05% Triton X-100 for 5 min on ice, followed by immunostaining with anti-PI4KIIα. Cells were also directly stained, with or without the permeabilization step, using 50 μg/ml filipin III (Sigma) for 20 min at room temperature.

Filipin III-labeled samples were imaged using a Zeiss LSM 510 Meta laser-scanning confocal microscope system essentially as described (29) using 405 nm line for excitation of filipin III. We also used a wide-field fluorescence system consisting of a Leica DMIRB inverted microscope equipped with a heated chamber and an Imago QE CCD camera. Filipin III was excited using a Polychrome IV xenon arc light source tuned to 360 nm (Till Photonics GmbH, Gräfelfing, Germany). The use of this system reduced photobleaching of filipin III fluorescence to negligible levels.

Imaging FRAP in eGFP-PI4KIIα-rich membranes

COS-7 cells were grown on 35 mm glass-bottomed dishes (Wilco-dish, Intracel, Royston, Herts, UK) and transiently transfected 24 h prior to imaging, with a construct encoding eGFP-PI4KIIα (29). FRAP was performed on a Zeiss LSM 510 Meta equipped with a heated stage maintained at 37°C. Cells were sterol depleted by incubation with MβCD for 20 min at 37°C in serum-free medium. Culture medium was replaced with Dulbecco's PBS containing 1 mM NaN_3 to completely inhibit the previously described intracellular trafficking of eGFP-PI4KIIα-positive vesicles (29). The use of NaN_3 in FRAP experiments to distinguish between vesicular and nonvesicular trafficking is well established (47). Furthermore, we found that while NaN_3 addition inhibited the movement of eGFP-PI4KIIα-containing vesicles, it did not induce any visible changes to the intracellular localization of eGFP-PI4KIIα. Therefore, NaN_3 addition permitted imaging of eGFP-PI4KIIα lateral diffusion without any fluorescence changes caused by the intracellular trafficking of PI4KIIα.

Prior to imaging FRAP, eGFP-PI4KIIα-rich membranes located in the juxtanuclear region were picked from randomly chosen transfectants (cells expressing high levels of eGFP-PI4KIIα were excluded). A circular area (0.7–1.0 μm in diameter) was then selectively photobleached with 60 iterative rounds of illumination with the 488 nm line from a 30 mW Argon laser (Lasos Lasertechnik, Jena, Germany) set to 50% output and 100% transmission. Recovery of the fluorescence signal in this spot was monitored by acquiring 12-bit images at 0.5 s intervals over a time course of 120 s, with the laser power reduced to 0. 9% transmission and with the pinhole fully open. To control unintentional photobleaching during the time course, an area from an adjacent cell with similar diameter and fluorescence intensity was scanned in parallel without the initial photobleaching. Photobleaching during the time course was negligible, and it was not necessary to correct the FRAP data. All data were collected using a C-Apochromat 63×/1.2 water immersion objective (Carl Zeiss). For analysis of membrane connectivity, fluorescence changes were monitored in an unbleached spot of equal area situated 3 μM away from the photobleached spot used for FRAP analysis.

FRAP data were exported from Zeiss LSM 5 software and analyzed using GraphPad Prism 4 curve fitting software. The diffusion coefficient (D) for eGFP-PI4KIIα was calculated as: $e^2.r^2/4\tau_{1/2}$ where r is the radius of the photobleached spot and $\tau_{1/2}$ is the half-time for maximal recovery of fluorescence after photobleaching (48).

The mobile fraction of eGFP-PI4KIIα was calculated as: $F(\infty)-F(0)/F(t<0)-F(0)$ where $F(t<0)$ is the fluorescence prior to photobleaching, $F(0)$ refers to residual fluorescence measured immediately after photobleaching, and $F(\infty)$ is maximal fluorescence recovery after photobleaching (48). Both $F(\infty)$ and $\tau_{1/2}$ were obtained by plotting fluorescence against time in seconds and by nonlinear regression curve fitting to a rectangular hyperbola desc ∞ ribed as: $F = F(\infty)\cdot t/\tau_{1/2} + t$.

RESULTS

Cholesterol modulates PI substrate availability to PI4KIIα

The PI 4-kinase activity associated with the buoyant TGN membrane fraction used in this study has been previously characterized and shown to be solely accounted for by PI4KIIα (5, 31, 36, 37). In the absence of detergent, PI4KIIα in this membrane fraction can phosphorylate PI added in the form of small unilamellar vesicles (SUV) (48). We observed that MβCD profoundly inhibited membrane-associated PI4P synthesis across a broad range (0–100 μM) of added PI substrate (**Fig. 1A**). In the presence of MβCD, PI4P synthesis was half-maximal at 3.5 μM PI, which was not significantly different from the half-maximal concentration of PI measured in the absence of MβCD (5, 36). Therefore, MβCD inhibited PI4KIIα without any apparent change in PI substrate affinity. This raised the possibility that sterol depletion inhibited PI4P synthesis through effects on either protein diffusion and/or membrane organization.

Non-cholesterol sterols and PI4KIIα activity

We previously demonstrated that the add-back of MβCD-complexed cholesterol can restore PI4P synthesis subsequent to cholesterol depletion by MβCD (5). For the current study, we used MβCD to replenish sterol-depleted PI4KIIα-rich membranes with noncholesterol sterols (Fig. 1B). The purpose of these experiments was to probe the molecular properties of sterols required to support intracellular

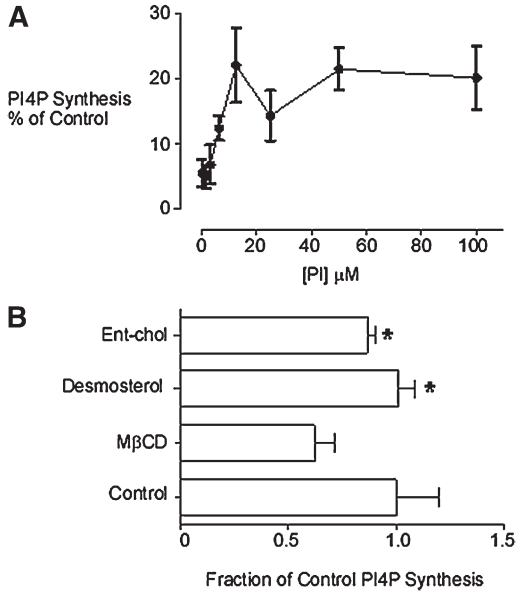

Fig. 1. A: MβCD inhibition of PI4KIIα. A buoyant membrane fraction enriched for PI4KIIα activity and TGN markers was prepared by equilibrium density gradient ultracentrifugation of postnuclear supernatants from COS-7 cells. Membranes were sterol-depleted with MβCD (10 mM) and [^{32}P]PI4P production determined in the presence of added PI (0–100 μM). B: Desmosterol and enantiomeric-cholesterol can support PI4KIIα-catalyzed PI phosphorylation. Equal volume aliquots of a TGN membrane fraction were sterol-depleted with MβCD and [^{32}P]PI4P production measured in the presence of either desmosterol or enantiomeric cholesterol added in complex with MβCD. *$P < 0.05$ compared with MβCD-pretreated samples. The final concentration of MβCD in these assays was equivalent to the IC_{50} concentration for inhibition of PI4P synthesis. MβCD, methyl-β-cyclodextrin; PI, phosphatidylinositol; PI4KII, type II phosphatidylinositol 4-kinase; PI4P, phosphatidylinositol 4-phosphate; TGN, *trans*-Golgi network.

PI4KIIα activity at the TGN. First we used MβCD as a vehicle to substitute native membrane-associated cholesterol for its mirror-image molecule enantiomeric cholesterol, which does not occur naturally. Enantiomeric cholesterol (46, 49, 50) possesses the same physicochemical properties as cholesterol in model membranes but cannot effectively substitute for native cholesterol in processes involving direct protein:cholesterol interactions (46, 51, 52). We also investigated if membrane-associated PI4KIIα activity could be supported by desmosterol rather than cholesterol. Desmosterol is an immediate metabolic precursor of cholesterol that differs only by one double bond at the C24 position. Despite its structural similarity to cholesterol, desmosterol is much less effective in stabilizing liquid-ordered membrane domains (53). We found that both desmosterol and enantiomeric cholesterol could enhance [^{32}P]PI4P synthesis following sterol depletion (Fig. 1B). Furthermore, these data show that an enantiomeric or structurally specific cholesterol binding is not required for the activation of PI4KIIα, which instead depends on membrane biophysical properties.

Relationship between membrane microdomains and PI4KIIα localization

To explore the idea that inhibition of PI4KIIα activity by MβCD was associated with a change in membrane organization, we evaluated the effects of MβCD on PI4KIIα compartmentation within TGN membranes (**Fig. 2**). As an assay for membrane microdomain heterogeneity, we used probe sonication to physically fragment a TGN-rich membrane fraction, followed by discontinuous equilibrium ultracentrifugation to separate the resultant membrane fragments on the basis of buoyant density (54, 55). Our previous analyses revealed that sonication consistently results in the formation of vesicles of diameter 70–200 nm (37, 56) and that this treatment also physically destroys any residual membrane network connectivity. We investigated the effects of MβCD on the distribution of cholesterol in the TGN gradient fractions. In gradients prepared from control membranes, cholesterol measured using the Amplex red cholesterol assay exhibited a broad asymmetric gradient distribution, with a main peak in gradient fraction 6 and gradually tailing off into the denser fractions (Fig. 2A). As expected, MβCD reduced the overall sterol content of the membranes by 70%. However, most of this loss was from the buoyant broad peak of cholesterol in the 5–30% sucrose interface of the density gradient. The residual cholesterol was all localized to a minor pool peaking in fraction 9–11 of the gradient (Fig. 2A). We also investigated the effects of cholesterol depletion on the gradient distribution syntaxin-6, a protein that, similar to PI4KIIα, has been shown to associate with TGN microdomains (57, 58) (Fig. 2B). We found that the MβCD addition resulted in a shift of syntaxin-6 protein from the 30% sucrose layer to the 30–40% sucrose interface. These results clearly show that MβCD treatment resulted in a reduction in the sterol content and buoyancy of a subset of TGN membranes and that this density shift is most likely due to the increased protein:lipid ratio of the sterol-depleted fractions.

To investigate the relationship between PI4KIIα targeting to cholesterol-rich membranes and enzyme activity, we assayed PI4P synthesis using exogenous micellar PI substrate in the presence of TX-100 detergent. These assay conditions completely solubilize PI4KIIα (31), and endogenous membrane-associated PI is diluted to such an extent that it does not contribute toward the measured PI4P production (31). Therefore, these assay conditions report PI4KIIα activity outside the membrane environment. For control membranes (n = 3), the gradient distribution of PI4KIIα activity closely followed the distribution of PI4KIIα protein, with a broad peak between fractions 6 and 8 corresponding to the 30% sucrose layer (Fig. 2C). Treatment with MβCD resulted in a marked loss of PI4KIIα protein from the 30% sucrose layer. In control gradients, 45.5 ± 3.6% (n = 3) of the total PI4KIIα protein was associated with the buoyant fraction, and subsequent to MβCD addition, this was significantly decreased to 11.7 ± 3.5% (n = 3). Loss of PI4KIIα protein was coupled with a loss of PI4KIIα activity from the buoyant fraction. However, sterol depletion did not result in an overall significant decrease in the total amount of PI4KIIα activity measured across all the gradient fractions. Therefore, changes to microdomain

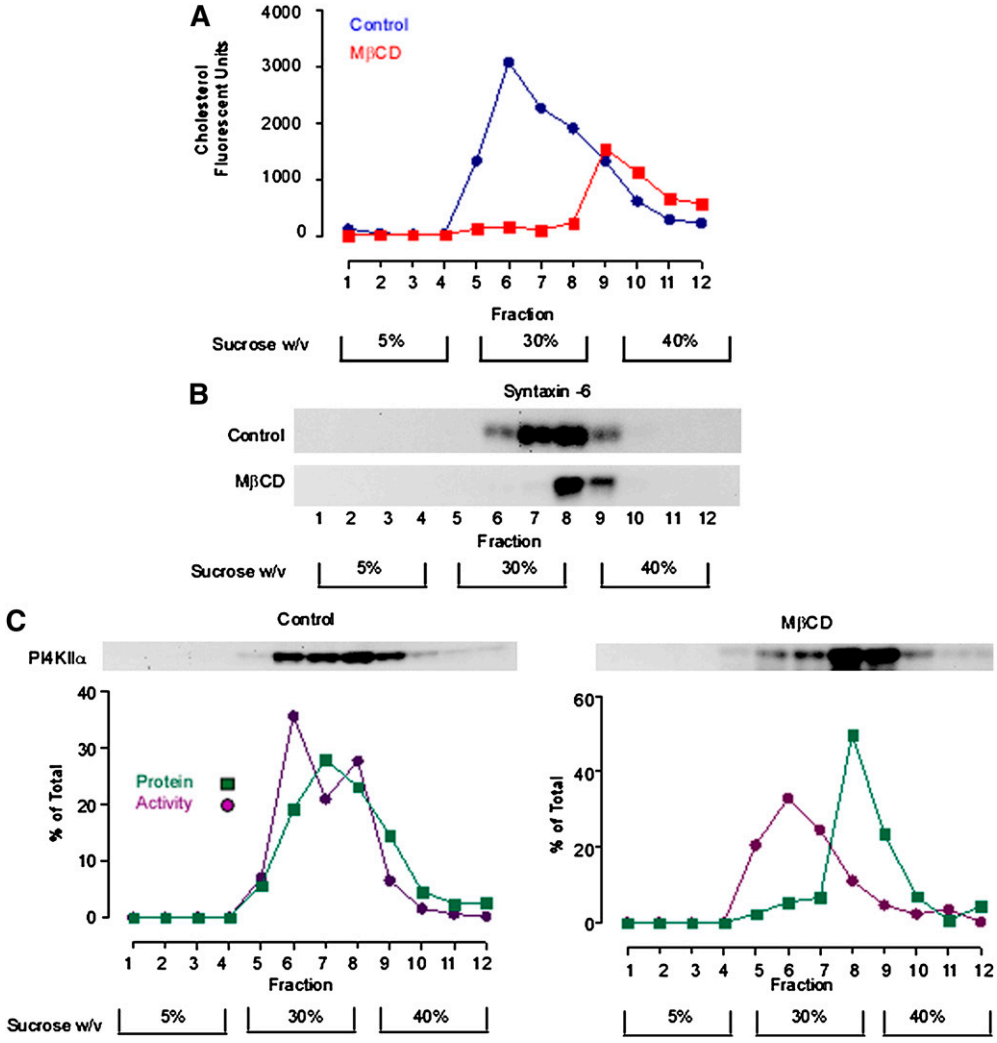

Fig. 2. MβCD alters the steady-state compartmentation of PI4KIIα. A TGN-enriched membrane fraction was probe sonicated and subfractionated in a discontinuous sucrose density gradient. A: The cholesterol content of equal volume aliquots from each gradient fraction was determined using the Amplex Red cholesterol assay. B: Anti-syntaxin 6 Western blot demonstrating the gradient distribution of syntaxin-6 in control and sterol-depleted membrane fractions. C: Gradient distribution of PI4KIIα protein and activity. Equal volume samples from each density gradient fraction were Western blotted and probed with an anti-PI4KIIα antibody. PI4KIIα activity associated with each fraction was determined by solubilizing the membranes and measuring [^{32}P]PI4P synthesis using a fixed concentration of micellar PI. PI4KIIα protein levels were determined by quantitative analysis of anti-PI4KIIα Western blots. Specific PI4KIIα activity associated with each fraction was calculated by dividing the rate of PI4P generation (phosphorimager units.min^{-1}) by the amount of PI4KIIα protein present in each fraction as determined by Western blotting (arbitrary units). The results presented here are representative of three independent experiments. MβCD, methyl-β-cyclodextrin; PI4KII, type II phosphatidylinositol 4-kinase; PI4P, phosphatidylinositol 4-phosphate.

lipid composition delocalize PI4KIIα to a different biophysical environment but do not change the intrinsic activity of the enzyme. These results also demonstrate that removal of PI4KIIα from the membrane environment by detergent solubilization abrogates its sterol sensitivity, suggesting that PI4KIIα is only sterol-sensitive within the context of the native membrane.

Colocalization of PI4KIIα and cholesterol

Results from the density gradient assays demonstrated overlap between cholesterol and PI4KIIα-rich regions of the TGN. To validate this result, we imaged the distribution of cholesterol with filipin III and compared it to the intracellular distribution of endogenous PI4KIIα by fluorescence microscopy (**Fig. 3**). Cholesterol was visualized on several different cellular membranes, including pronounced staining at the plasma membrane. PI4KIIα staining was more restricted to intracellular vesicles with very little staining at the plasma membrane. Our membrane fractionation data indicated that PI4KIIα distributed between membranes of differing cholesterol content. Differential colocalization of PI4KIIα with cholesterol was also observed in these imaging experiments, where both overlapping and nonoverlapping pools of PI4KIIα and cholesterol were visible in the juxtanuclear region of individual cells.

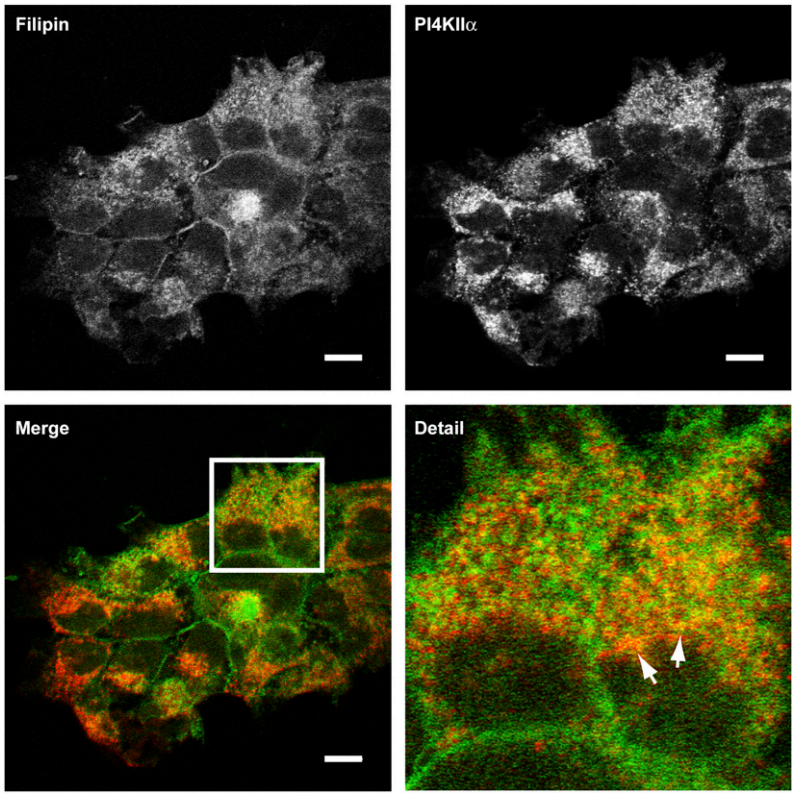

Fig. 3. Distribution of sterol and endogenous PI4KIIα in A431 cells. Fixed cells were costained with filipin III (green channel) and an anti-PI4KIIα monoclonal antibody (red channel) and imaged by confocal microscopy. Arrows indicate membranes in the jutanuclear region with the greatest colocalization of filipin and PI4KIIα. Scale bars 10 μm. Images are representative of three independent experiments. PI4KII, type II phosphatidylinositol 4-kinase.

MβCD treatment affects the morphology of PI4KIIα-rich membranes

We investigated the effects of sterol depletion with MβCD on the intracellular localization of PI4KIIα. In these experiments, we used confocal imaging to examine the effect of sterol depletion on eGFP-PI4KIIα and filipin III staining to image cholesterol. Under both control and cholesterol-depleted conditions, eGFP-PI4KIIα localized primarily to juxtanuclear intracellular vesicles (**Fig. 4**). Addition of MβCD induced two visible changes to the juxtanuclear pool of eGFP-PI4KIIα. First, the TGN pool of the enzyme contracted in size by up to 50%, and second, there was a visible vesicularization of the eGFP-PI4KIIα-containing membranes. These observations are consistent with the previously described effects of MβCD on TGN membranes (24, 43, 44). In addition, MβCD treatment had dramatic effects on cellular sterol levels as imaged by filipin staining (Fig. 4). Under these experimental conditions and notwithstanding some residual filipin staining in the juxtanuclear region, MβCD treatment resulted in large losses of filipin staining throughout the cell.

Imaging the effects of MβCD treatment on colocalization of PI4KIIα with TGN marker proteins

Our imaging of the intracellular distribution of eGFP-PI4KIIα following sterol depletion was consistent with MβCD-induced changes to TGN morphology. This led us to consider the degree to which reductions in membrane sterol levels and subsequent changes to Golgi architecture might affect the colocalization of PI4KIIα with the TGN proteins TGN46 and syntaxin-6 (**Fig. 5**). In cholesterol-replete cells, there was extensive overlap between eGFP-PI4KIIα and syntaxin-6, and this overlap was maintained following sterol depletion. In control cells, there was limited overlap between TGN46 and eGFP-PI4KIIα, and this partial colocalization was completely lost in the presence of MβCD. These results demonstrate that the juxtanuclear pool of eGFP-PI4KIIα corresponds to a syntaxin-6-positive subdomain of the TGN. However, as syntaxin-6 has been localized to both the TGN and postTGN vesicles, it is more accurate to refer these membranes as a TGN-endosomal compartment.

FRAP experiments on cells expressing GFP-PI4KIIα

As sterol depletion induced the redistribution of PI4KIIα to membrane compartments with differing biophysical properties and protein mobility can be modulated by membrane sterol content (6–10), we decided to investigate whether addition of MβCD influenced PI4KIIα lateral diffusion. To measure the dynamics of PI4KIIα within cell membranes, FRAP experiments were carried out on COS-7 cells transiently transfected with GFP-PI4KIIα. We have previously determined that PI4KIIα-containing vesicles undergo rapid intracellular trafficking (29). To differentiate between FRAP caused by membrane trafficking events from that resulting solely from eGFP-PI4KIIα lateral diffusion, we carried out experiments in cells which had been azide-treated to deplete cellular ATP and thereby inhibit energy-dependent vesicular trafficking (47). In these experiments, a spot of diameter 0.7–1.0 μM was photobleached and fluorescence recovery was measured at 0.5 s intervals over a 100–200 s time course. To standardize between different

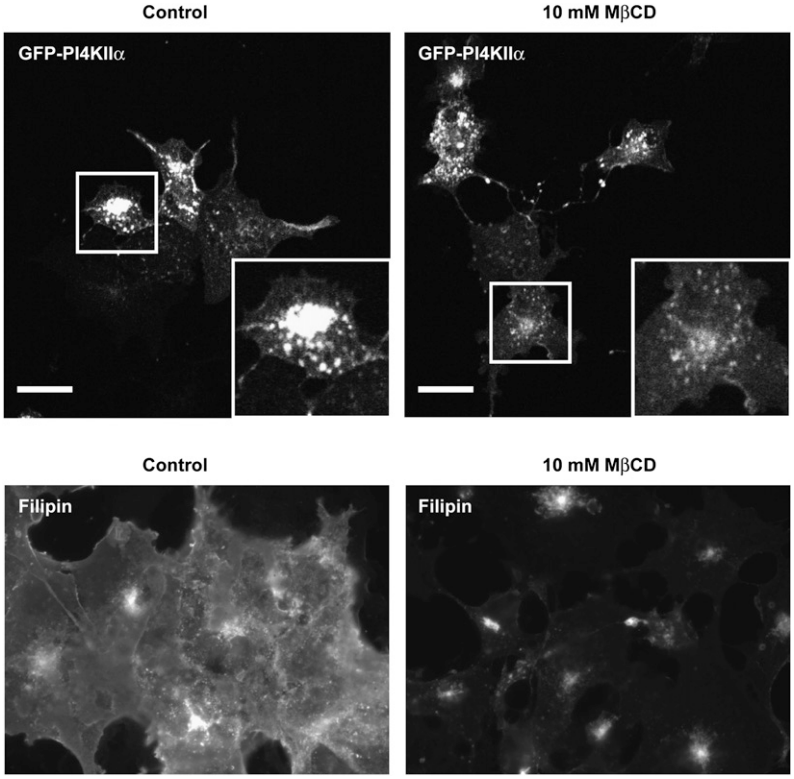

Fig. 4. The effects of MβCD treatment on eGFP-PI4KIIα and sterol distribution. Cells expressing eGFP-PI4KIIα were treated with 10 mM MβCD for 20 min, fixed, and imaged by confocal microscopy. Boxed regions show detail of typical cells. Scale bar 20 μm. Cells treated with and without MβCD were also fixed and stained with filipin III and imaged by wide-field fluorescence microscopy to determine the extent of sterol depletion. Control images were collected to 12-bit peak, and identical gain settings were used in MβCD-treated cells. Images are representative of three independent experiments. eGFP, enhanced green fluorescent protein; MβCD, methyl-β-cyclodextrin; PI4KII, type II phosphatidylinositol 4-kinase.

photobleaching experiments, we took care to choose spots of average fluorescence intensity and always from eGFP-PI4KIIα-positive vesicular structures in the juxtanuclear region of the cells (**Fig. 6A**). Typically, photobleaching of control eGFP-PI4KIIα membranes resulted in a steady recovery of eGFP-PI4KIIα fluorescence over a 2 min time course with a diffusion coefficient (D) of $0.87 \pm 0.3 \times 10^{-9}$ $cm^2.s^{-1}$ (n = 6) and with 55.5 ± 11.2% (n = 6) of the protein mobile (Fig. 6B). We are confident that these measurements reflect lateral diffusion since trial experiments revealed that the diffusion coefficient was linear with respect to the bleached spot area. However, for MβCD-treated cells, the mobile fraction dropped to 30.9 ± 6.3% (n = 6) while D was increased at $2.4 \pm 1.0 \times 10^{-9}$ $cm^2.s^{-1}$ (n = 6). The relatively large error in the calculated D value probably reflects the heterogeneous effects of MβCD on TGN morphology that we observed for the juxtanuclear eGFP-PI4KIIα compartment. It is has been reported that factors such as membrane topology and geometry can have a large effects on calculated D values (59, 60). However, despite this complication, in four out of six paired experiments the apparent D value for eGFP-PI4KIIα was increased following MβCD treatment. As regards the effects of MβCD on the mobile fraction of eGFP-PI4KIIα, overall fluorescence recovery was reduced by sterol depletion in six out of six paired experiments. Similarly, the half-time for fluorescence recovery ($\tau_{1/2}$) on control membranes was 26.5 ± 10.8 s (n = 6) compared with 8.4 ± 3.5 s (n = 6) for sterol-depleted membranes. In summary, our FRAP analysis revealed that MβCD treatment induced significant changes to the mobility of eGFP-PI4KIIα on TGN-endosomal membranes.

Our analysis of the distribution of the juxtanuclear pool of eGFP-PI4KIIα demonstrated that the TGN-endosome membranes appeared more vesicular after addition of MβCD. This led us to examine whether such a loss of membrane continuity could affect the dynamics of eGFP-PI4KIIα.We again used the spot photobleaching approach to determine the extent to which PI4KIIα was free to diffuse throughout the TGN-endosome compartment. To do this, we monitored fluorescence changes in an identically sized but unbleached spot 3–4 μm away from the photobleached spot (Fig. 6C). The reasoning behind this approach was that fluorescence changes in the unbleached spot require exchange of eGFP-PI4KIIα with the photobleached area by lateral diffusion. Therefore, changes in fluorescence in the unbleached spot report connectivity changes between different regions of the membrane. In control TGN membranes, we observed that fluorescence loss and recovery in the unbleached spot closely followed the pattern of FRAP in the photobleached spot, although the magnitudes of such changes were reduced. However, addition of MβCD resulted in a loss of fluorophore movement between both areas, thereby revealing a loss of diffusion-based connectivity between both regions of the membrane. These results demonstrate that the reduction in overall recovery of eGFP-PI4KIIα subsequent to sterol depletion results from a marked loss of continuity in TGN-endosomal membranes.

DISCUSSION

The key findings of this study are that sterol depletion with MβCD induces physical changes to TGN-endosomal membranes, resulting in decreased PI4KIIα

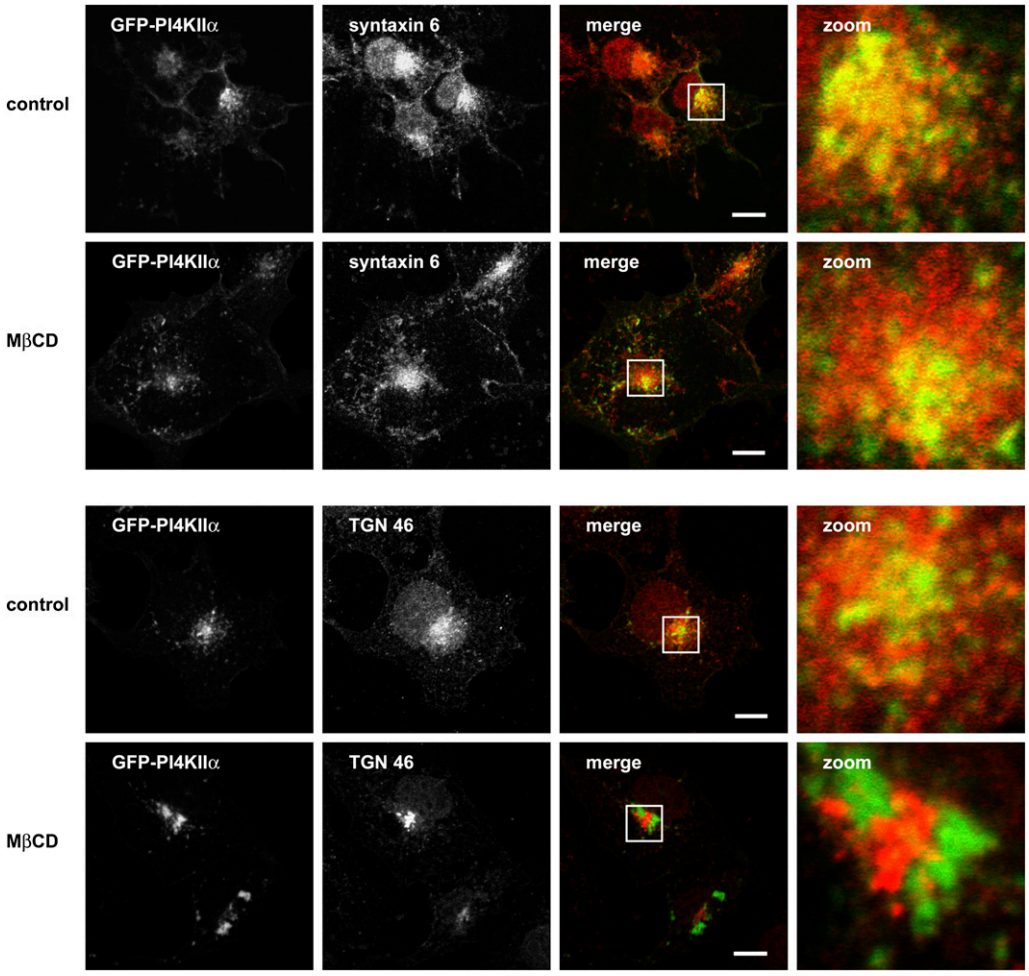

Fig. 5. eGFP-PI4KIIα colocalizes with TGN markers in the juxtanuclear region of the cell. Cells expressing eGFP-PI4KIIα (green) were fixed and immunostained with antibodies to either syntaxin-6 or TGN46 (red) in the presence or absence MβCD 10 mM. The boxed areas show detail of the PI4KIIα and TGN marker-positive membranes used in FRAP experiments. Note that colocalization of syntaxin-6 and eGFP-PI4KIIα is maintained after sterol depletion. Images are representative of three independent experiments. eGFP, enhanced green fluorescent protein; FRAP, fluorescence recovery after photobleaching; MβCD, methyl-β-cyclodextrin; PI4KII, type II phosphatidylinositol 4-kinase; TGN, *trans*-Golgi network.

activity. Reduction in membrane cholesterol also induces a loss of TGN membrane continuity and a concomitant reduction in the PI4KIIα mobile fraction. This leads us to conclude that cholesterol-dependent compartmentation of PI4KIIα affects the dynamics of the enzyme and that this is important for PI4P generation.

Note that our analyses of PI4KIIα distribution on sterol-depleted membranes, both by membrane fractionation and by fluorescence imaging, demonstrated that cholesterol is not absolutely required for association of the enzyme with the membrane. Furthermore, membrane association alone does not facilitate PI4P synthesis, as this is dependent on the membrane cholesterol content. In this regard, the ability of enantiomeric cholesterol to functionally substitute for native cholesterol in enhancing PI4P formation is a key finding. This is because cholesterol chirality does not affect spontaneous membrane domain formation or noncovalent interactions with other lipids (46, 61). Cholesterol chirality is, however, important for cholesterol-protein binding, as this tends to be an enantiospecific process (46, 52, 62). Therefore, the ability to restore PI4KIIα activity with enantiomeric cholesterol implies an indirect role for sterols in modulating PI4P synthesis through effects on membrane organization. We also found that even in instances where PI substrate is present in high concentrations, PI4KIIα activity was inhibited in the presence of MβCD. This further strengthens the idea that cholesterol modulates PI4P synthesis indirectly by facilitating the interaction of PI4KIIα with its phospholipid substrate. Our membrane subfractionation studies demonstrated that MβCD treatment led to a major loss of cholesterol from a pool of TGN-endosomal membranes, a concomitant collapse in membrane microdomain heterogeneity, and delocalization of PI4KIIα to denser membrane fractions. This shift in buoyant density is the first evidence that a pool of PI4KIIα physically associates with cholesterol-rich membranes. Subsequent solubilization of the membrane fractions and assays for PI4P synthesis revealed that PI4KIIα intrinsic activity was not altered in cholesterol-depleted membranes. These data show that MβCD-induced changes to membrane domain heterogeneity

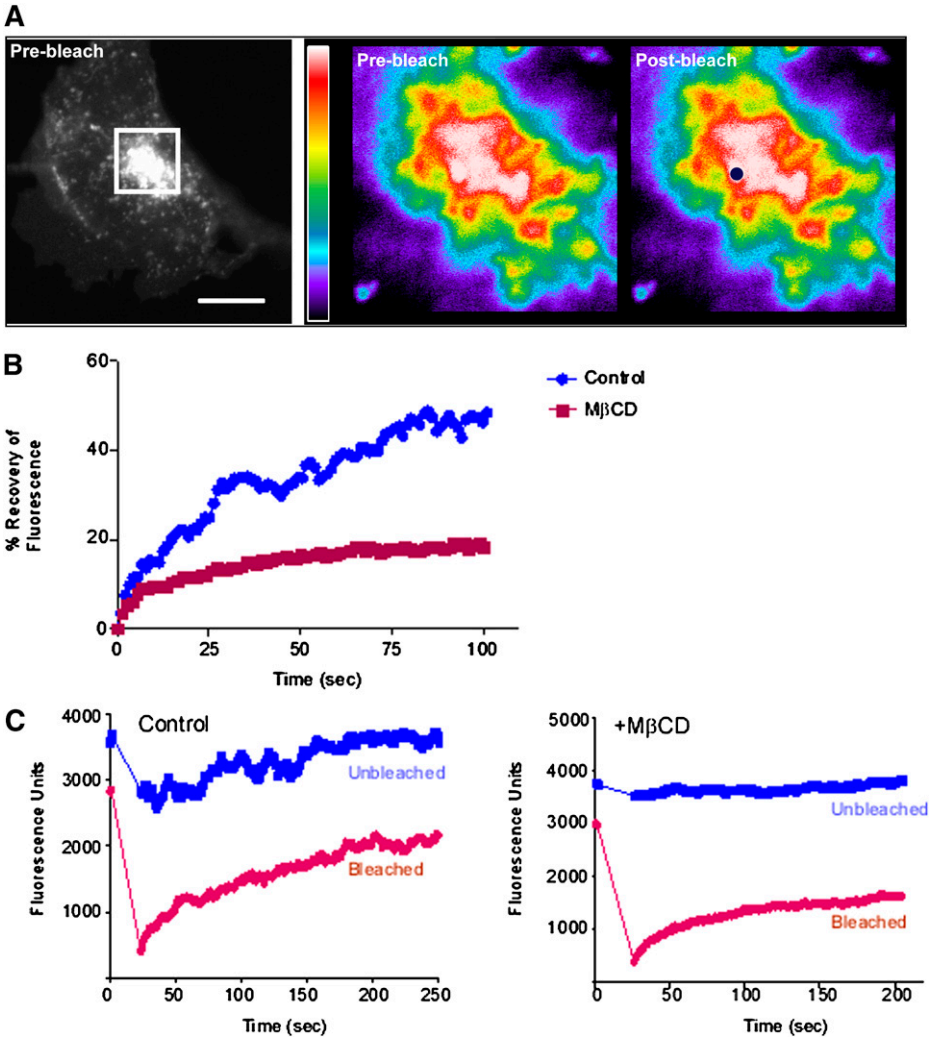

Fig. 6. FRAP analysis of eGFP-PI4KIIα on juxtanuclear membranes. A: Illustration of the FRAP scheme. Membranes in the juxtanuclear area of live eGFP-PI4KIIα-expressing cells (boxed) were selectively photobleached in a circular region of interest (ROI). The rate of recovery of fluorescence in such ROIs was then followed over a time course in azide-treated cells, with and without MβCD pretreatment. Scale bar 10 μm. B: FRAP recovery curves for eGFP-PI4KIIα obtained from control and sterol-depleted cells. C: MβCD addition causes loss of TGN membrane continuity. Comparison of fluorescence changes for photobleached and unbleached spots situated 3 μm apart and in the same TGN membrane for control and MβCD-treated cells. All experiments were repeated at least six times with similar results. eGFP, enhanced green fluorescent protein; FRAP, fluorescence recovery after photobleaching; MβCD, methyl-β-cyclodextrin; PI4KII, type II phosphatidylinositol 4-kinase; TGN, *trans*-Golgi network.

correlate with a decrease in productive interactions between PI4KIIα and PI. This is consistent with an important role for membrane cholesterol in maintaining PI4P generation through effects on membrane organization.

MβCD treatment results in a decreased mobile fraction of eGFP-PI4KIIα, and this implies an important role for the TGN-endosomal cholesterol concentration in determining the overall mobility of the protein. While previous work demonstrated that a fraction of total cellular PI4KIIα associates with detergent-insoluble membrane domains (31), it does not necessarily mean that targeting of the protein-to-lipid rafts is the underlying explanation for the results we present here. Moreover, other studies have shown that the relationship between protein mobility and association with lipid rafts is not straightforward. As an example, some have reported mobility differences between raft proteins and nonraft-associated proteins and suggested that proteins targeted to a single type of raft diffuse together as small entities (63, 64). This differs from others who concluded that differences in protein mobility do not necessarily reflect confinement to lipid rafts (65). In the case of PI4KIIα, the differences in protein mobility that we observed can be rationalized by overall MβCD-induced changes to membrane morphology and connectivity (24, 43, 44) without the need to invoke the targeting of PI4KIIα to lipid rafts. In particular, our photobleaching analysis demonstrated that MβCD-induced changes to membrane structure limit the pool of fluorophore available to replenish the photobleached spot, and this manifests as a reduced mobile fraction of eGFP-PI4KIIα.

The increase in the size of the immobile PI4KIIα fraction following sterol depletion has some similarities with the scenario described for palmitoylation-deficient mutants of PI4KIIα that are membrane localized but inactive (38). Consistent with more recent work (35), we also find that palmitoylation-deficient versions of PI4KIIα are not targeted to the TGN (unpublished observations), which precludes an investigation into the relationship between PI4KIIα palmitoylation and mobility on juxtanuclear membranes. However, our work is consistent with a model proposed by Barylko et al. (35) in which dynamic regulation of PI4KIIα palmitoylation underlies PI4P synthesis at the TGN. This leads us to suggest that, in common with palmitoylated Ras protein at the TGN (66, 67), palmitoylation-dependent targeting of PI4KIIα to cholesterol-rich membrane domains kinetically traps the protein in this compartment and that this is the biochemical mechanism underlying sterol-modulated PI4P generation on intracellular membranes.

The authors acknowledge Royal Free NHS Trust support of the Advanced Microscopy Unit used in these studies.

REFERENCES

1. Balla, A., and T. Balla. 2006. Phosphatidylinositol 4-kinases: old enzymes with emerging functions. *Trends Cell Biol.* **16:** 351–361.
2. Simons, J. P., R. Al-Shawi, S. Minogue, M. G. Waugh, C. Wiedemann, S. Evangelou, A. Loesch, T. S. Sihra, R. King, T. T. Warner, et al. 2009. Loss of phosphatidylinositol 4-kinase 2alpha activity causes late onset degeneration of spinal cord axons. *Proc. Natl. Acad. Sci. USA.* **106:** 11535–11539.
3. Wang, Y. J., J. Wang, H. Q. Sun, M. Martinez, Y. X. Sun, E. Macia, T. Kirchhausen, J. P. Albanesi, M. G. Roth, and H. L. Yin. 2003. Phosphatidylinositol 4 phosphate regulates targeting of clathrin adaptor AP-1 complexes to the Golgi. *Cell.* **114:** 299–310.
4. Li, J., Y. Lu, J. Zhang, H. Kang, Z. Qin, and C. Chen. 2010. PI4KIIalpha is a novel regulator of tumor growth by its action on angiogenesis and HIF-1alpha regulation. *Oncogene.* **29:** 2550–2559.
5. Waugh, M. G., S. Minogue, D. Chotai, F. Berditchevski, and J. J. Hsuan. 2006. Lipid and peptide control of phosphatidylinositol 4-kinase IIalpha activity on Golgi-endosomal rafts. *J. Biol. Chem.* **281:** 3757–3763.
6. Owen, D. M., D. Williamson, C. Rentero, and K. Gaus. 2009. Quantitative microscopy: protein dynamics and membrane organisation. *Traffic.* **10:** 962–971.
7. Adkins, E. M., D. J. Samuvel, J. U. Fog, J. Eriksen, L. D. Jayanthi, C. B. Vaegter, S. Ramamoorthy, and U. Gether. 2007. Membrane mobility and microdomain association of the dopamine transporter studied with fluorescence correlation spectroscopy and fluorescence recovery after photobleaching. *Biochemistry.* **46:** 10484–10497.
8. Baier, C. J., C. E. Gallegos, V. Levi, and F. J. Barrantes. 2010. Cholesterol modulation of nicotinic acetylcholine receptor surface mobility. *Eur Biophys J.* **39:** 213–227.
9. Ma, X., Q. Wang, Y. Jiang, Z. Xiao, X. Fang, and Y. G. Chen. 2007. Lateral diffusion of TGF-beta type I receptor studied by single-molecule imaging. *Biochem. Biophys. Res. Commun.* **356:** 67–71.
10. Vrljic, M., S. Y. Nishimura, W. E. Moerner, and H. M. McConnell. 2005. Cholesterol depletion suppresses the translational diffusion of class II major histocompatibility complex proteins in the plasma membrane. *Biophys. J.* **88:** 334–347.
11. Lingwood, D., H. J. Kaiser, I. Levental, and K. Simons. 2009. Lipid rafts as functional heterogeneity in cell membranes. *Biochem. Soc. Trans.* **37:** 955–960.
12. Pike, L. J. 2004. Lipid rafts: heterogeneity on the high seas. *Biochem. J.* **378:** 281–292.
13. Eggeling, C., C. Ringemann, R. Medda, G. Schwarzmann, K. Sandhoff, S. Polyakova, V. N. Belov, B. Hein, C. von Middendorff, A. Schonle, et al. 2009. Direct observation of the nanoscale dynamics of membrane lipids in a living cell. *Nature.* **457:** 1159–1162.
14. Coxey, R. A., P. G. Pentchev, G. Campbell, and E. J. Blanchette-Mackie. 1993. Differential accumulation of cholesterol in Golgi compartments of normal and Niemann-Pick type C fibroblasts incubated with LDL: a cytochemical freeze-fracture study. *J. Lipid Res.* **34:** 1165–1176.
15. Orci, L., R. Montesano, P. Meda, F. Malaisse-Lagae, D. Brown, A. Perrelet, and P. Vassalli. 1981. Heterogeneous distribution of filipin—cholesterol complexes across the cisternae of the Golgi apparatus. *Proc. Natl. Acad. Sci. USA.* **78:** 293–297.
16. van Meer, G., D. R. Voelker, and G. W. Feigenson. 2008. Membrane lipids: where they are and how they behave. *Nat. Rev. Mol. Cell Biol.* **9:** 112–124.
17. Balla, A., G. Tuymetova, A. Tsiomenko, P. Varnai, and T. Balla. 2005. A plasma membrane pool of phosphatidylinositol 4-phosphate is generated by phosphatidylinositol 4-kinase type-III alpha: studies with the PH domains of the oxysterol binding protein and FAPP1. *Mol. Biol. Cell.* **16:** 1282–1295.
18. Hammond, G. R., G. Schiavo, and R. F. Irvine. 2009. Immunocytochemical techniques reveal multiple, distinct cellular pools of PtdIns4P and PtdIns(4,5)P(2). *Biochem. J.* **422:** 23–35.
19. Levine, T. P., and S. Munro. 2002. Targeting of Golgi-specific pleckstrin homology domains involves both PtdIns 4-kinase-dependent and -independent components. *Curr. Biol.* **12:** 695–704.
20. Weixel, K. M., A. Blumental-Perry, S. C. Watkins, M. Aridor, and O. A. Weisz. 2005. Distinct Golgi populations of phosphatidylinositol 4-phosphate regulated by phosphatidylinositol 4-kinases. *J. Biol. Chem.* **280:** 10501–10508.
21. De Matteis, M. A., A. Di Campli, and A. Godi. 2005. The role of the phosphoinositides at the Golgi complex. *Biochim. Biophys. Acta.* **1744:** 396–405.
22. Di Paolo, G., and P. De Camilli. 2006. Phosphoinositides in cell regulation and membrane dynamics. *Nature.* **443:** 651–657.
23. Wang, J., H. Q. Sun, E. Macia, T. Kirchhausen, H. Watson, J. S. Bonifacino, and H. L. Yin. 2007. PI4P promotes the recruitment of the GGA adaptor proteins to the trans-Golgi network and regulates their recognition of the ubiquitin sorting signal. *Mol. Biol. Cell.* **18:** 2646–2655.
24. Hansen, G. H., L. L. Niels-Christiansen, E. Thorsen, L. Immerdal, and E. M. Danielsen. 2000. Cholesterol depletion of enterocytes. Effect on the Golgi complex and apical membrane trafficking. *J. Biol. Chem.* **275:** 5136–5142.
25. Klemm, R. W., C. S. Ejsing, M. A. Surma, H. J. Kaiser, M. J. Gerl, J. L. Sampaio, Q. de Robillard, C. Ferguson, T. J. Proszynski, A. Shevchenko, et al. 2009. Segregation of sphingolipids and sterols during formation of secretory vesicles at the trans-Golgi network. *J. Cell Biol.* **185:** 601–612.
26. Wang, Y., C. Thiele, and W. B. Huttner. 2000. Cholesterol is required for the formation of regulated and constitutive secretory vesicles from the trans-Golgi network. *Traffic.* **1:** 952–962.
27. Balla, T., and P. Varnai. 2002. Visualizing cellular phosphoinositide pools with GFP-fused protein-modules. *Sci. STKE.* **2002:** P13.
28. Craige, B., G. Salazar, and V. Faundez. 2008. Phosphatidylinositol-4-kinase type II alpha contains an AP-3-sorting motif and a kinase domain that are both required for endosome traffic. *Mol. Biol. Cell.* **19:** 1415–1426.
29. Minogue, S., M. G. Waugh, M. A. De Matteis, D. J. Stephens, F. Berditchevski, and J. J. Hsuan. 2006. Phosphatidylinositol 4-kinase is required for endosomal trafficking and degradation of the EGF receptor. *J. Cell Sci.* **119:** 571–581.
30. Salazar, G., B. Craige, B. H. Wainer, J. Guo, P. De Camilli, and V. Faundez. 2005. Phosphatidylinositol-4-kinase type II alpha is a component of adaptor protein-3-derived vesicles. *Mol. Biol. Cell.* **16:** 3692–3704.
31. Waugh, M. G., S. Minogue, D. Blumenkrantz, J. S. Anderson, and J. J. Hsuan. 2003. Identification and characterization of differentially active pools of type IIalpha phosphatidylinositol 4-kinase activity in unstimulated A431 cells. *Biochem. J.* **376:** 497–503.
32. Berger, A. C., G. Salazar, M. L. Styers, K. A. Newell-Litwa, E. Werner, R. A. Maue, A. H. Corbett, and V. Faundez. 2007. The subcellular localization of the Niemann-Pick Type C proteins depends on the adaptor complex AP-3. *J. Cell Sci.* **120:** 3640–3652.
33. Bock, J. B., J. Klumperman, S. Davanger, and R. H. Scheller. 1997. Syntaxin 6 functions in trans-Golgi network vesicle trafficking. *Mol. Biol. Cell.* **8:** 1261–1271.

34. Banting, G., and S. Ponnambalam. 1997. TGN38 and its orthologues: roles in post-TGN vesicle formation and maintenance of TGN morphology. *Biochim. Biophys. Acta.* **1355:** 209–217.
35. Barylko, B., Y. S. Mao, P. Wlodarski, G. Jung, D. D. Binns, H. Q. Sun, H. L. Yin, and J. P. Albanesi. 2009. Palmitoylation controls the catalytic activity and subcellular distribution of phosphatidylinositol 4-kinase II{alpha}. *J. Biol. Chem.* **284:** 9994–10003.
36. Waugh, M. G., S. Minogue, J. S. Anderson, A. Balinger, D. Blumenkrantz, D. P. Calnan, R. Cramer, and J. J. Hsuan. 2003. Localization of a highly active pool of type II phosphatidylinositol 4-kinase in a p97/valosin-containing-protein-rich fraction of the endoplasmic reticulum. *Biochem. J.* **373:** 57–63.
37. Waugh, M. G., D. Lawson, S. K. Tan, and J. J. Hsuan. 1998. Phosphatidylinositol 4-phosphate synthesis in immunoisolated caveolae-like vesicles and low buoyant density non-caveolar membranes. *J. Biol. Chem.* **273:** 17115–17121.
38. Barylko, B., S. H. Gerber, D. D. Binns, N. Grichine, M. Khvotchev, T. C. Sudhof, and J. P. Albanesi. 2001. A novel family of phosphatidylinositol 4-kinases conserved from yeast to humans. *J. Biol. Chem.* **276:** 7705–7708.
39. Jung, G., J. Wang, P. Wlodarski, B. Barylko, D. D. Binns, H. Shu, H. L. Yin, and J. P. Albanesi. 2008. Molecular determinants of activation and membrane targeting of phosphoinositol 4-kinase IIbeta. *Biochem. J.* **409:** 501–509.
40. Zidovetzki, R., and I. Levitan. 2007. Use of cyclodextrins to manipulate plasma membrane cholesterol content: evidence, misconceptions and control strategies. *Biochim. Biophys. Acta.* **1768:** 1311–1324.
41. Naveen, B., B. S. Shankar, and G. Subrahmanyam. 2005. FcepsilonRI cross-linking activates a type II phosphatidylinositol 4-kinase in RBL 2H3 cells. *Mol. Immunol.* **42:** 1541–1549.
42. Pike, L. J., and J. M. Miller. 1998. Cholesterol depletion delocalizes phosphatidylinositol bisphosphate and inhibits hormone-stimulated phosphatidylinositol turnover. *J. Biol. Chem.* **273:** 22298–22304.
43. Stuven, E., A. Porat, F. Shimron, E. Fass, D. Kaloyanova, B. Brugger, F. T. Wieland, Z. Elazar, and J. B. Helms. 2003. Intra-Golgi protein transport depends on a cholesterol balance in the lipid membrane. *J. Biol. Chem.* **278:** 53112–53122.
44. Grimmer, S., T. G. Iversen, B. van Deurs, and K. Sandvig. 2000. Endosome to Golgi transport of ricin is regulated by cholesterol. *Mol. Biol. Cell.* **11:** 4205–4216.
45. Lebreton, S., S. Paladino, and C. Zurzolo. 2008. Selective roles for cholesterol and actin in compartmentalization of different proteins in the Golgi and plasma membrane of polarized cells. *J. Biol. Chem.* **283:** 29545–29553.
46. Westover, E. J., D. F. Covey, H. L. Brockman, R. E. Brown, and L. J. Pike. 2003. Cholesterol depletion results in site-specific increases in epidermal growth factor receptor phosphorylation due to membrane level effects. Studies with cholesterol enantiomers. *J. Biol. Chem.* **278:** 51125–51133.
47. Hao, M., S. X. Lin, O. J. Karylowski, D. Wustner, T. E. McGraw, and F. R. Maxfield. 2002. Vesicular and non-vesicular sterol transport in living cells. The endocytic recycling compartment is a major sterol storage organelle. *J. Biol. Chem.* **277:** 609–617.
48. Goodwin, J. S., and A. K. Kenworthy. 2005. Photobleaching approaches to investigate diffusional mobility and trafficking of Ras in living cells. *Methods.* **37:** 154–164.
49. Westover, E. J., and D. F. Covey. 2003. First synthesis of ent-desmosterol and its conversion to ent-deuterocholesterol. *Steroids.* **68:** 159–166.
50. Westover, E. J., and D. F. Covey. 2004. The enantiomer of cholesterol. *J. Membr. Biol.* **202:** 61–72.
51. Crowder, C. M., E. J. Westover, A. S. Kumar, R. E. Ostlund, Jr., and D. F. Covey. 2001. Enantiospecificity of cholesterol function in vivo. *J. Biol. Chem.* **276:** 44369–44372.
52. Zitzer, A., E. J. Westover, D. F. Covey, and M. Palmer. 2003. Differential interaction of the two cholesterol-dependent, membrane-damaging toxins, streptolysin O and Vibrio cholerae cytolysin, with enantiomeric cholesterol. *FEBS Lett.* **553:** 229–231.
53. Megha, B. O., and E. London. 2006. Cholesterol precursors stabilize ordinary and ceramide-rich ordered lipid domains (lipid rafts) to different degrees. Implications for the Bloch hypothesis and sterol biosynthesis disorders. *J. Biol. Chem.* **281:** 21903–21913.
54. Smart, E. J., Y. S. Ying, C. Mineo, and R. G. Anderson. 1995. A detergent-free method for purifying caveolae membrane from tissue culture cells. *Proc. Natl. Acad. Sci. USA.* **92:** 10104–10108.
55. Song, K. S., S. Li, T. Okamoto, L. A. Quilliam, M. Sargiacomo, and M. P. Lisanti. 1996. Co-purification and direct interaction of Ras with caveolin, an integral membrane protein of caveolae microdomains. Detergent-free purification of caveolae microdomains. *J. Biol. Chem.* **271:** 9690–9697.
56. Waugh, M. G., D. Lawson, and J. J. Hsuan. 1999. Epidermal growth factor receptor activation is localized within low-buoyant density, non-caveolar membrane domains. *Biochem. J.* **337:** 591–597.
57. Vetrivel, K. S., H. Cheng, S. H. Kim, Y. Chen, N. Y. Barnes, A. T. Parent, S. S. Sisodia, and G. Thinakaran. 2005. Spatial segregation of gamma-secretase and substrates in distinct membrane domains. *J. Biol. Chem.* **280:** 25892–25900.
58. Vetrivel, K. S., H. Cheng, W. Lin, T. Sakurai, T. Li, N. Nukina, P. C. Wong, H. Xu, and G. Thinakaran. 2004. Association of gamma-secretase with lipid rafts in post-Golgi and endosome membranes. *J. Biol. Chem.* **279:** 44945–44954.
59. Sbalzarini, I. F., A. Mezzacasa, A. Helenius, and P. Koumoutsakos. 2005. Effects of organelle shape on fluorescence recovery after photobleaching. *Biophys. J.* **89:** 1482–1492.
60. Sukhorukov, V. M., and J. Bereiter-Hahn. 2009. Anomalous diffusion induced by cristae geometry in the inner mitochondrial membrane. *PLoS ONE.* **4:** e4604.
61. Alakoskela, J. M., K. Sabatini, X. Jiang, V. Laitala, D. F. Covey, and P. K. Kinnunen. 2008. Enantiospecific interactions between cholesterol and phospholipids. *Langmuir.* **24:** 830–836.
62. Covey, D. F. 2009. ent-Steroids: novel tools for studies of signaling pathways. *Steroids.* **74:** 577–585.
63. Meder, D., M. J. Moreno, P. Verkade, W. L. Vaz, and K. Simons. 2006. Phase coexistence and connectivity in the apical membrane of polarized epithelial cells. *Proc. Natl. Acad. Sci. USA.* **103:** 329–334.
64. Pralle, A., P. Keller, E. L. Florin, K. Simons, and J. K. Horber. 2000. Sphingolipid-cholesterol rafts diffuse as small entities in the plasma membrane of mammalian cells. *J. Cell Biol.* **148:** 997–1008.
65. Kenworthy, A. K., B. J. Nichols, C. L. Remmert, G. M. Hendrix, M. Kumar, J. Zimmerberg, and J. Lippincott-Schwartz. 2004. Dynamics of putative raft-associated proteins at the cell surface. *J. Cell Biol.* **165:** 735–746.
66. Goodwin, J. S., K. R. Drake, C. L. Remmert, and A. K. Kenworthy. 2005. Ras diffusion is sensitive to plasma membrane viscosity. *Biophys. J.* **89:** 1398–1410.
67. Goodwin, J. S., K. R. Drake, C. Rogers, L. Wright, J. Lippincott-Schwartz, M. R. Philips, and A. K. Kenworthy. 2005. Depalmitoylated Ras traffics to and from the Golgi complex via a nonvesicular pathway. *J. Cell Biol.* **170:** 261–272.